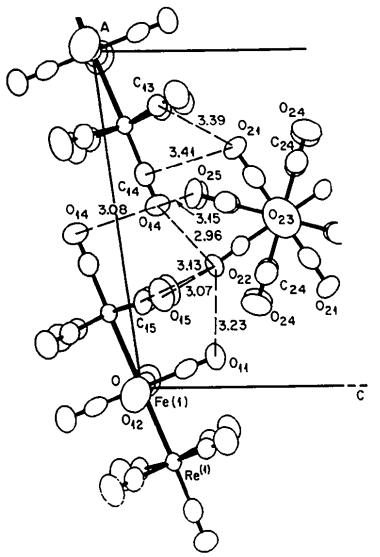

Fig. 2. A perspective drawing along the *b* axis of molecules 1 and 2 showing significant interatomic distances (Å).

the extent of backbonding is influenced by the van der Waals distances, perhaps dominated by the short O(23)···O(23) approach.

This research was sponsored by the Division of Material Sciences, Office of Basic Energy Sciences, US Department of Energy, under contract DE-AC05-840R21400 with Martin Marietta Energy Systems, Inc.

References

AGRON, P. A., ELLISON, R. D. & LEVY, H. A. (1967). *Acta Cryst.* **23**, 1079–1086.
AGRON, P. A., ELLISON, R. D. & LEVY, H. A. (1968). Report ORNL-4306, pp. 157–160. Oak Ridge National Laboratory, Tennessee, USA.
AGRON, P. A., ELLISON, R. D. & LEVY, H. A. (1988). *Am. Crystallogr. Assoc. Meet. Abstr.* **16**, PE16.
BAILEY, M. F. & DAHL, L. F. (1965). *Inorg. Chem.* **4**, 1140–1144.
BRAGA, D. & KOETZLE, T. F. (1987). *J. Chem. Soc. Chem. Commun.* pp. 608–610.
BRAGA, D. & KOETZLE, T. F. (1988). *Acta Cryst.* B**44**, 151–155.
BUSING, W. R., ELLISON, R. D., KING, S. P., LEVY, H. A. & ROSEBERRY, R. T. (1968). Report ORNL-4143. Oak Ridge National Laboratory, Tennessee, USA.
BUSING, W. R. & LEVY, H. A. (1957). *Acta Cryst.* **10**, 180–182.
BUSING, W. R. & LEVY, H. A. (1964). *Acta Cryst.* **17**, 142–146.
CHURCHILL, M. R., AMOH, K. N. & WASSERMAN, H. J. (1981). *Inorg. Chem.* **20**, 1609–1611.
COTTON, F. A. & DANIELS, L. M. (1983). *Acta Cryst.* C**39**, 1495–1496.
CROCKER, L. S., MATTSON, B. M., HEINEKEY, D. M. & SCHULTE, G. K. (1988). *Inorg. Chem.* **27**, 3722–3729.
DAHL, L. F. & RUNDLE, R. E. (1963). *Acta Cryst.* **16**, 419–426.
EVANS, G. O. & SHELINE, R. K. (1971). *Inorg. Chem.* **10**, 1598–1605.
HAMILTON, W. C. (1959). *Acta Cryst.* **12**, 609–610.
MARTIN, M., REES, B. & MITSCHLER, A. (1982). *Acta Cryst.* B**38**, 6–15.

Acta Cryst. (1991). C**47**, 916–919

Refinement of the Structure of Liroconite, a Heteropolyhedral Framework Oxysalt Mineral

BY PETER C. BURNS, RAY K. EBY* AND FRANK C. HAWTHORNE

Department of Geological Sciences, University of Manitoba, Winnipeg, Manitoba, Canada R3T 2N2

(*Received* 10 *August* 1990; *accepted* 1 *October* 1990)

Abstract. Aluminium dicopper arsenate tetrahydroxide tetrahydrate, $Cu_2Al(AsO_4)(OH)_4.4H_2O$, M_r = 433, monoclinic, $I2/a$, a = 12·664 (2), b = 7·563 (2), c = 9·914 (3) Å, β = 91·32 (2)°, V = 949·4 (3) Å^3, Z = 4, D_x = 3·04 g cm^{-3}, λ(Mo $K\alpha$) = 0·71073 Å, μ = 84·9 cm^{-1}, $F(000)$ = 848, T = 297 K, R = 0·027 for 1215 observed reflections. The structure is a heteropolyhedral framework of $[AsO_4]$ tetrahedra, $[CuO_2(OH)_2(H_2O)_2]$ octahedra and $[AlO_2(OH)_4]$ octahedra.

Introduction. We have a systematic study of the stereochemistry of Cu^{2+} oxysalt minerals currently under way (Eby & Hawthorne, 1989*a*,*b*; Hawthorne & Eby, 1985; Hawthorne & Groat, 1985, 1986; Hawthorne, 1985*a*,*b*, 1986*a*,*b*; Groat & Hawthorne, 1987; Hawthorne, Groat & Eby, 1989) focused primarily on the heteropolyhedral connectivity of these structures and the interaction between local Jahn–Teller distortion, polyhedral connectivity and structural periodicity. As part of this work a refinement and reconsideration of the structure of clinoclase was initiated.

* Present address: Department of Geological Sciences, University of New Mexico, Albuquerque, New Mexico 87131, USA.

0108-2701/91/050916-04$03.00

Experimental. Liroconite from Roughton Gill, England, National Mineral Collection catalogue number 18291, was obtained from the Royal Ontario Museum. Crystal size: ground sphere 0·24 mm; unit-cell parameters refined from 25 reflections automatically aligned on a Nicolet *R3m* diffractometer at 297 K. Data collection: 1386 reflections; $3 < 2\theta < 60°$; h −16–16, k 0–10, l 0–13; graphite monochromator, Mo $K\alpha$ X-radiation; $\theta/2\theta$ scan, variable scan speed 4·0–29·3° min^{-1}, scan range ($K\alpha_1 - 1$)→($K\alpha_2 + 1$)°, background/scan = 0·5; two standard reflections every 48 reflections, variation 2·0%; absorption correction by ψ-scan method (minimum transmission 0·081, maximum transmission 0·113); Lorentz and polarization corrections; 1215 observed reflections with $I > 3\sigma I$. Structure refinement: atomic scattering factors and anomalous-dispersion coefficients from *International Tables for X-ray Crystallography* (1974, Vol. IV); all calculations performed with *SHELXTL* (Sheldrick, 1981) on a Nova 4S computer. Starting parameters from Kolesova & Fesenko (1968), refinement by full-matrix least squares (on F) with anisotropic temperature factors converged to $R = 0·027$, $wR = 0·027$, $w = 1$, $S = 2·08$; maximum final shift/e.s.d. < 0·05, mean < 0·01; maximum height in final difference Fourier map = 0·70 e Å^{-3}.

Discussion. Fractional coordinates and equivalent isotropic temperature factors of atoms in the asymmetric unit are listed in Table 1* and interatomic distances and angles are given in Table 2. The As atom is tetrahedrally coordinated by O atoms but the mean bond length of 1·660 Å is significantly less than that typically observed in arsenate structures. This suggests substitution of a smaller cation for As^{5+} at the tetrahedral site. Qualitative electron-microprobe analysis by energy-dispersive spectrometry showed the presence of significant phosphorus in addition to copper, aluminium and arsenic, with an As:P ratio of ~0·80:0·20. This substitution is in accord with the short ⟨As—O⟩ distance observed here. With the assumption of ideal ⟨As—O⟩ and ⟨P—O⟩ distances of 1·685 and 1·536 Å, respectively (Griffen & Ribbe, 1979), the ⟨As—O⟩ distance of 1·660 Å observed here gives an As:P ratio of 0·83:0·17, close to that indicated by the electron-microprobe data. The site occupancy of the As site was also refined; assuming substitution by P, the resulting occupancy ratio was 0·83:0·17. The As:P ratio is similar by all three methods of estimation and indicates significant P

* Lists of structure factors and anisotropic displacement parameters have been deposited with the British Library Document Supply Centre as Supplementary Publication No. SUP 53613 (6 pp.). Copies may be obtained through The Technical Editor, International Union of Crystallography, 5 Abbey Square, Chester CH1 2HU, England.

Table 1. *Atomic parameters and equivalent isotropic temperature factors* (Å^2 × 10^4) *for liroconite*

$U_{eq} = (1/3)\Sigma_i\Sigma_j U_{ij} a_i^* a_j^* \mathbf{a}_i.\mathbf{a}_j.$

	x	y	z	U_{eq}
Cu	0·13090 (3)	0·22187 (6)	0·27026 (4)	137 (1)
As	¼	0·04570 (7)	0	95 (1)
Al	0	0	0	111 (4)
O(1)	0·8558 (2)	0·0801 (4)	0·0063 (3)	197 (7)
O(2)	0·2457 (2)	0·1734 (4)	0·1380 (2)	197 (7)
OH(1)	0·0244 (2)	0·0959 (4)	0·1736 (2)	227 (7)
OH(2)	0·0410 (2)	0·2238 (4)	0·9229 (2)	190 (7)
O*W*(1)	0·6843 (3)	0·1195 (5)	0·3405 (4)	473 (12)
O*W*(2)	0·1104 (3)	0·4922 (5)	0·1206 (3)	334 (9)

Table 2. *Interatomic distances* (Å) *and angles* (°) *in liroconite*

As—O(1^{iii})	1·644 (3)		Cu—O(2)		2·014 (2)
As—O(2^{iii})	1·676 (3)		Cu—O(2^{viii})		1·957 (2)
⟨As—O⟩	1·660		Cu—OH(1)		1·894 (3)
			Cu—OH(2^{ix})		1·958 (2)
Al—O(1^{i,iv})	1·926 (2)		Cu—O*W*(1^{ii})		2·754 (4)
Al—OH(1^{v})	1·886 (3)		Cu—O*W*(2)		2·536 (3)
Al—OH(2^{vi,vii})	1·933 (3)		⟨Cu—O⟩[4]		1·956
⟨Al—O⟩	1·915		⟨Cu—O⟩[6]		2·186
O(1^{i})—As—O(1^{iii})		109·3 (2)	O(1^{i})—O(1^{iii})		2·681 (5)
O(1^{i})—As—O(2)	×2	108·8 (1)	O(1^{i})—O(2)	×2	2·700 (4)
O(1^{i})—As—O(2^{iii})	×2	110·1 (1)	O(1^{i})—O(2^{iii})	×2	2·722 (4)
O(2)—As—O(2^{iii})		109·7 (2)	O(2)—O(2^{iii})		2·740 (5)
⟨O—As—O⟩		109·5	⟨O—O⟩As		2·711
O(1^{i})—Al—OH(1)	×2	90·9 (1)	O(1)—OH(1)	×2	2·716 (4)
O(1^{i})—Al—OH(1^{v})	×2	89·1 (1)	O(1)—OH(1^{v})	×2	2·675 (3)
O(1^{i})—Al—OH(2^{vi})	×2	89·9 (1)	O(1)—OH(2^{vi})	×2	2·728 (4)
O(1^{i})—Al—OH(2^{vii})	×2	90·1 (1)	O(1)—OH(2^{vii})	×2	2·730 (4)
OH(1)—Al—OH(2^{vii})	×2	89·1 (1)	OH(1)—OH(2^{vi})	×2	2·679 (4)
OH(1)—Al—OH(2^{vii})	×2	90·9 (1)	OH(1)—OH(2^{vii})	×2	2·722 (4)
⟨O—Al—O⟩		90·0	⟨O—O⟩Al		2·708
O(2)—Cu—O(2^{viii})		78·2 (1)	O(2)—O(2^{viii})		2·506 (5)
O(2)—Cu—OH(1)		95·5 (1)	O(2)—OH(1)		2·893 (4)
O(2)—Cu—O*W*(1^{ii})		79·5 (1)	O(2)—O*W*(1^{ii})		3·101 (5)
O(2)—Cu—O*W*(2)		80·3 (1)	O(2)—O*W*(2)		2·961 (4)
O(2^{viii})—Cu—OH (2^{ix})		91·6 (1)	O(2^{viii})—OH(2^{ix})		2·807 (3)
O(2^{viii})—Cu—O*W*(1^{ii})		94·2 (1)	O(2^{viii})—O*W*(1^{ii})		3·493 (5)
O(2^{viii})—Cu—O*W*(2)		90·9 (1)	O(2)^{viii}—O*W*(2)		3·228 (5)
OH(1)—Cu—OH(2^{ix})		94·4 (1)	OH(1)—OH(2^{ix})		2·827 (4)
OH(1)—Cu—O*W*(1^{ii})		79·9 (1)	OH(1)—O*W*(1^{ii})		3·056 (5)
OH(1)—Cu—O*W*(2)		92·7 (1)	OH(1)—O*W*(2)		3·236 (5)
OH(2^{ix})—Cu—O*W*(1^{ii})		98·3 (1)	OH(2^{ix})—O*W*(1^{ii})		3·602 (5)
OH(2^{ix})—Cu—O*W* (2)		103·3 (1)	OH(2^{ix})—O*W*(2)		3·543 (5)
⟨O—Cu—O⟩		89·9	⟨O—O⟩Cu		3·104
OH(1)—O*W*(2^{x})	2·802 (3)		O*W*(2)—OH(2^{vi})		2·942 (4)
OH(2)—O*W*(2^{xi})	2·905 (4)		O*W*(2)—O*W*(1^{xiii})		2·791 (4)
O*W*(1)—O(1^{xii})	2·786 (3)				

Symmetry code: (i): $1-x, -y, -z$; (ii): $-\frac{1}{2}+x, -y, z$; (iii): $\frac{1}{2}-x, y, -z$; (iv): $-1+x, y, z$; (v): $-x, -y, -z$; (vi): $x, y, -1+z$; (vii): $-x, -y, 1-z$; (viii) $\frac{1}{2}-x, \frac{1}{2}-y, \frac{1}{2}-z$; (ix): $x, \frac{1}{2}-y, -\frac{1}{2}+z$; (x): $-x, -\frac{1}{2}+y, \frac{1}{2}-z$; (xi): $-x, 1-y, 1-z$; (xii): $\frac{3}{2}-x, \frac{1}{2}-y, \frac{1}{2}-z$; (xiii): $1-x, \frac{1}{2}+y, \frac{1}{2}-z$.

Table 3. *Bond-valence table for liroconite*

	Cu	Al	As	H(1)	H(2)	H(3)	H(4)	H(5)	H(6)	Sum
O(1)		0·476 × 2	1·315 × 2			0·18				1·971
O(2)	0·384		1·207 × 2							2·063
	0·472									
OH(1)	0·559	0·530 × 2		0·82						1·909
OH(2)	0·470	0·467 × 2			0·87				0·15	1·957
O*W*(1)	0·055					0·82	1·00	0·18		2·055
O*W*(2)	0·099			0·18	0·13			0·82	0·85	2·079
	2·039	2·964	5·044	1·00	1·00	1·00	1·00	1·00	1·00	

substitution into the ideal $Cu_2Al(AsO_4)(OH)_4(H_2O)_4$ liroconite structure. The bond-valence distribution (Table 3) was calculated using the parameters of Brown & Altermatt (1985); note that the bond-valence sum closely approaches the ideal value of 5·0 v.u. when the site occupancy (0·83 As + 0·17 P) is used. Summation of the bond valencies around the anions shows a significant deficiency at the O(1) atom position (0·476 + 1·315 = 1·791 v.u.) suggesting a fairly strong hydrogen bond to O(1); the only reasonable donor–acceptor distance is 2·786 Å for O(1)···O*W*(1) with a corresponding H(1)···O(1) bond valence of 0·18 v.u. to give a satisfactory sum of 1·971 v.u. around O(1). The local geometry suggests the hydrogen-bond system indicated in Table 3, which results in a reasonable set of bond-valence sums around both cations and anions in the structure.

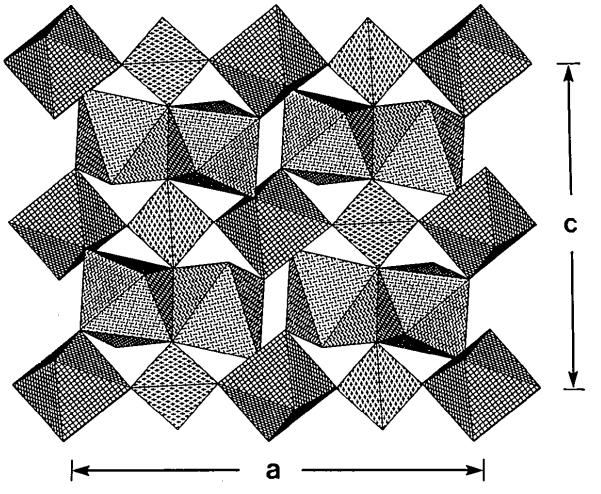

Fig. 1. The structure of liroconite projected onto (010); AsO_4 tetrahedra are shaded by crosses, AlO_6 octahedra are shaded by a 4^4 net and CuO octahedra are dash-shaded.

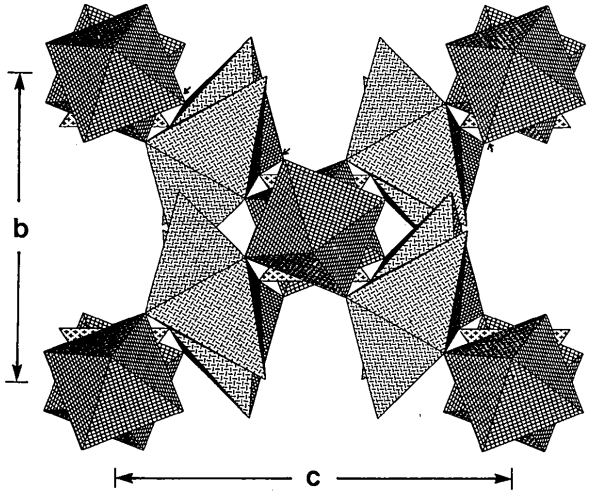

Fig. 2. The structure of liroconite projected onto (100); legend as in Fig. 1, linkages marked by arrows are displaced one cell translation along [100].

The Al atom is surrounded by two O atoms and four hydroxyl groups in an octahedral arrangement, with the O atoms in a *trans* configuration; there is only minor distance and angle deviation from their ideal holosymmetric values. The Cu^{2+} ion is coordinated by two O atoms, two hydroxyls and two H_2O groups; the O atoms are in a *cis* configuration, the hydroxyl groups are in a *cis* configuration and the H_2O groups are in a *trans* configuration. The Cu^{2+} ion has a very distorted octahedral coordination geometry. The four short meridional distances ($\langle$[4]Cu—O$\rangle$ = 1·956 Å) and two long axial distances ($\langle^{axial}$Cu − O$\rangle$ = 2·645 Å) are typical of the (4+2)-type Jahn–Teller distortion caused by the intrinsic orbital instability of an ideal holosymmetric $[Cu^{2+}O_6]$ octahedral complex with respect to a symmetry-lowering deformation.

A (010) projection of the structure is shown in Fig. 1. An important motif of the structure is the linear $[Al(AsO_4)\varphi_4]$ chain (φ = unspecified ligand) extending along [001]. In the (100) projection (Fig. 2), these chains lie at the corners and at the centre of the unit cell and neighbouring octahedra along the chain (linked through a common arsenate group) are twisted approximately 90° from each other. The other key feature of the structure is the $[Cu_2O_2(OH)_4(H_2O)_4]$ edge-sharing dimer that is well illustrated in Fig. 1. The octahedra share their O—O edge and through these O atoms link to the arsenate groups of adjacent chains, satisfying the local bond-valence requirements of these atoms in the process (Table 3). The two hydroxyl groups form the ends of the dimer and cross link to the $[AlO_6]$ octahedra whereas the two H_2O groups form the elongated apical Cu—O bonds and are only hydrogen bonded to other polyhedra. The cross linkage of the chains is also seen in Fig. 2, in which the Jahn–Teller-type (4 + 2) distortion of the $[Cu\varphi_6]$ octahedra is very apparent.

Financial support was provided by the Natural Sciences and Engineering Research Council of Canada; the Council is thanked for Graduate Fellowships for PCB and RKE, a University Research Fellowship, an Operating Grant, a Major Equipment Grant and an Infrastructure Grant to FCH.

References

Brown, I. D. Altermatt, D. (1985). *Acta Cryst.* B**41**, 244–247.
Eby, R. K. & Hawthorne, F. C. (1989*a*). *Acta Cryst.* C**45**, 1479–1482.
Eby, R. K. & Hawthorne, F. C. (1989*b*). *Mineral. Petrol.* **40**, 127–136.

GRIFFEN, D. T. & RIBBE, P. H. (1979). *Neues Jahrb. Mineral. Abh.* **137**, 54–73.
GROAT, L. A. & HAWTHORNE, F. C. (1987). *Tschermaks Mineral. Petrogr. Mitt.* **37**, 87–96.
HAWTHORNE, F. C. (1985*a*). *Mineral. Mag.* **49**, 85–91.
HAWTHORNE, F. C. (1985*b*). *Tschermaks Mineral Petrogr. Mitt.* **34**, 15–34.
HAWTHORNE, F. C. (1986*a*). *Can. Mineral.* **24**, 625–642.
HAWTHORNE, F. C. (1986*b*). *Am. Mineral.* **71**, 206–209.
HAWTHORNE, F. C. & EBY, R. K. (1985). *Neues Jahrb. Mineral. Monatsh.* pp. 234–240.
HAWTHORNE, F. C. & GROAT, L. A. (1985). *Am. Mineral.* **70**, 1050–1055.
HAWTHORNE, F. C. & GROAT, L. A. (1986). *Mineral. Mag.* **50**, 157–162.
HAWTHORNE, F. C., GROAT, L. A. & EBY, R. K. (1989). *Can. Mineral.* **27**, 205–209.
KOLESOVA, R. V. & FESENKO, E. G. (1968). *Sov. Phys. Crystallogr.* **13**, 324–328.
SHELDRICK, G. M. (1981). *Nicolet SHELXTL Operations Manual.* Revision 3. Nicolent XRD Corporation, Cupertino, California, USA.

Acta Cryst. (1991). C**47**, 919–924

Structure of $ZnGa_2S_4$, a Defect Sphalerite Derivative

BY CHARLOTTE K. LOWE-MA AND TERRELL A. VANDERAH

Chemistry Division of the Research Department, Naval Weapons Center, China Lake, CA 93555, USA

(*Received* 23 *August* 1989; *accepted* 9 *October* 1990)

Abstract. Digallium zinc tetrasulfide, $ZnGa_2S_4$, M_r = 333·07, tetragonal, $I\bar{4}2m$, a = 5·2744 (7), c = 10·407 (1) Å, V = 289·51 (9) Å^3, Z = 2, D_x = 3·82 g cm^{-3}, λ(Mo $K\alpha$) = 0·71069 Å, μ = 146·78 cm^{-1}, $F(000)$ = 312, T = 292 K. $ZnGa_2S_4$ crystallizes in the defect stannite structure which is related to sphalerite. Refinement of different models of cation distribution gave R values of 0·041 to 0·043 for 360 independent reflections with $|F_o| > 3\sigma(F)$. Of the models considered, the ordered model with Zn only at point set 2(*a*) and Ga only at point set 4(*d*) was found to be worse, statistically, than models with some degree of cation disorder. Models with cation disorder are consistent with a previous review in which it was suggested that the displacement of the anion from the ideal $(\frac{1}{4},\frac{1}{4},\frac{1}{8})$ was insufficient in $ZnGa_2S_4$ to indicate cation ordering. Disorder amongst the cation sites is also consistent with reported Raman and photoluminescence results. The slight difference observed between the metal–sulfur bond lengths for the two crystallographic cation sites is attributed to the differing effect of the vacancy on these sites rather than to cation ordering.

Introduction. Non-oxide inorganic compounds such as ternary sulfides and phosphides are of interest as possible infrared-transmitting window materials. $ZnGa_2S_4$ is of interest in second-phase toughening studies of ZnS (Zhang, Chen, Dunn & Ardell, 1988) and exhibits long-wavelength infrared transparency comparable to that of ZnS (Wu, He, Dwight & Wold, 1988; Gao, Wu, Kershaw, Dwight & Wold, 1989).

The title compound was first reported by Hahn, Frank, Klingler, Stoerger & Stoerger (1955). Hahn *et al.* (1955) postulated that the structure of $ZnGa_2S_4$ was that of an ordered defect sphalerite, the ordering of the vacancy and the two different cations giving rise to two possible structural arrangements, *A* and *B*, Fig. 1. These two arrangements cannot be distinguished by X-ray powder diffraction since the scattering factors for Zn and Ga are nearly identical. In the parent *AX* sphalerite structure each cation is tetrahedrally bonded to four anions and each anion is tetrahedrally bonded to four cations. The relationship between the sphalerite structure and the possible zinc thiogallate structures can be seen in Fig. 1. The (cubic) sphalerite cell has been doubled in one direction for ease of comparison to the thiogallate cell. In the thiogallate structure, one-quarter of the cations have been removed from the sphalerite structure in an ordered fashion, lowering the symmetry to tetragonal. This results in equivalent anion sites, each coordinated by one vacancy and three cations, while pseudo-tetrahedral coordination about each of the metal sites is preserved. The thiogallate structure has been considered as an ABX_2 defect chalcopyrite or defect stannite structure; the chalcopyrite and stannite structures are themselves ordered (tetragonal) versions of sphalerite but without vacancies. In the parent 'ideal' sphalerite the anion would be at (x,y,z) coordinates $(\frac{1}{4},\frac{1}{4},\frac{1}{4})$ or at $(\frac{1}{4},\frac{1}{4},\frac{1}{8})$ in a cell doubled in c. In these sphalerite derivatives the cations and vacancies occupy special positions; the anion position is specified by two or three coordinates x,x,z or x,y,z, that determine all of the metal–sulfur and vacancy–sulfur distances.

Despite the ease of growing crystals of $ZnGa_2S_4$ by iodine transport (Nitsche, Boelsterli & Lichtensteiger, 1961) a full single-crystal structure deter-

0108-2701/91/050919-06$03.00